



Effect of L-Shaped Shear Wall Layout on the Seismic Performance of Medium-Rise RC Buildings

Efecto de la disposición de muros de corte en forma de L sobre el comportamiento sísmico de edificios de hormigón armado de mediana altura

S. Merabti^{1*}, R. Hadj-Sadok², W. Zebboudj³

¹Laboratory of Acoustics and Civil Engineering, Faculty of Science and Technology, University Djilali Bounaama of Khemis-Miliana, Algeria, E-mail: s.merabti@univ.dbkm.dz

^{2,3}Faculty of Science and Technology, University Djilali Bounaama of Khemis-Miliana, Algeria

Received: 10/01/2026 | Accepted: 14/01/2026 | Publication date: 20/01/2026
DOI: 10.20868/abe.2025.3.5647

HIGHLIGHTS

- Model 4 exhibits the lowest shear, compression, and lateral displacements, indicating better force distribution.
- It limits critical stress concentrations at lintels and wall ends.
- It significantly reduces drifts and base shear, by up to 14 % and 16 % compared to other models.
- It provides an effective compromise between stiffness, force redistribution, and mitigation of critical demands.

TITULARES

- El Modelo 4 presenta los menores desplazamientos por cortante, compresión y acción lateral, lo que indica una mejor distribución de esfuerzos.
 - Limita las concentraciones críticas de tensiones en dinteles y extremos de muro.
 - Reduce de forma significativa las derivas y el cortante basal, con disminuciones de hasta un 14 % y un 16 %, respectivamente, en comparación con otros modelos.
 - Ofrece un compromiso óptimo entre rigidez, redistribución de esfuerzos y mitigación de demandas críticas.
-

RESUMEN

Este artículo investiga la influencia de la disposición de los muros de cortante en la respuesta sísmica de un edificio de mediana altura situado en una zona de alta sismicidad (Zona III), utilizando el software ETABS. Se analizan muros de cortante de hormigón armado en forma de L, diseñados para presentar una rigidez equivalente en ambas direcciones principales, bajo diferentes configuraciones de disposición. La evaluación comparativa se realiza a partir de indicadores habituales de la respuesta global frente a cargas laterales, incluyendo los desplazamientos laterales, el cortante en la base, el momento de vuelco y los niveles de tensiones en los muros de cortante. Los resultados ponen de manifiesto una mejora global del comportamiento sísmico cuando el sistema resistente a fuerzas laterales combina un núcleo central con muros de cortante dispuestos en las esquinas, en comparación con las demás configuraciones analizadas. En cambio, las disposiciones basadas únicamente en muros de cortante en forma de L ubicados en el perímetro resultan menos eficaces. Estos resultados permiten formular recomendaciones prácticas para un diseño sísmico optimizado.

Palabras clave: *Hormigón armado, edificio de mediana altura, muros de corte en forma de L, disposición de muros de corte, ETABS.*

ABSTRACT

This article investigates the influence of shear wall layout on the seismic response of a mid-rise building located in a high seismicity zone (Zone III) using ETABS software. Reinforced concrete L-shaped shear walls, designed to exhibit equivalent stiffness in both principal directions, are analyzed under several layout configurations. A comparative assessment is carried out based on standard global response indicators under lateral loading, including lateral displacements, base shear, overturning moment, and stress levels within the shear walls. The results highlight an overall improvement in seismic performance when the lateral force-resisting system combines a central core with corner-located shear walls, compared to the other configurations examined. In contrast, layouts relying solely on peripheral L-shaped shear walls prove to be less effective. These findings enable the formulation of practical recommendations for optimized seismic design.

Keywords: *Reinforced concrete, mid-rise building, L-shaped shear walls, shear wall layout, ETABS.*

1. INTRODUCTION

In reinforced concrete buildings, shear walls are among the most commonly used structural elements, as they provide an efficient and rational resistance to horizontal actions, particularly those induced by wind and earthquakes [1–5]. The widespread use of reinforced concrete shear walls imparts high stiffness to buildings due to their strong capacity to resist both horizontal and vertical loads [6, 7]. Consequently, reducing the number of shear walls may significantly alter the stiffness distribution and increase the overall flexibility of the structure, provided that adequate strength and stability levels required by design codes are maintained [8, 9]. In this context, structural engineering practice offers several strategies to limit excessive stiffness while preserving satisfactory structural performance, notably through optimized shear wall layout, adjustment of wall dimensions, and improved design of the lateral force-resisting system [10].

In recent years, L-shaped shear walls have emerged as an effective structural solution in reinforced concrete buildings, particularly when dictated by architectural constraints [11]. Owing to their geometry, these walls often allow better architectural integration and more flexible spatial arrangements, while ensuring adequate resistance to lateral loads and satisfactory global stiffness [12–14]. When properly designed and detailed, L-shaped shear walls can achieve structural strength and durability comparable to those of more conventional wall configurations [15]. Other wall shapes, such as U-, T-, L-, and H-shaped walls, may also be adopted; however, the L-shaped configuration has demonstrated favorable performance in buildings with various plan geometries [16, 17].

L-shaped shear walls have been widely discussed in the scientific literature. Several researchers have highlighted not only their structural relevance, but also their influence on the global behavior of buildings as a function of height [18, 19]. Merabti and Bezari [20] first provided a reliable overview of the concept of L-shaped shear walls. This work was subsequently extended by Ma et al. [21] and Ahmed-Chaouch et al. [22], who investigated the influence of wall slenderness and thickness on stress distribution. Furthermore, studies by Ozkula et al. [23] and Zhang et al. [24] demonstrated the benefits of L-shaped shear walls, as well as the positive effects of reinforcing steel enhancement in both longitudinal and transverse directions. Other authors, such as Yang et al. [25] and Zhou et al. [26], proposed lightweight concrete shear walls as an innovative alternative. In contrast, Ding et al. [27] employed ultra-high-performance concrete (UHPC) to improve energy dissipation and ductility of shear walls.

To highlight the influence of openings in shear walls on the seismic behavior of buildings, Kalpana et al. [28] examined the effects of the number and shape of openings, demonstrating that these parameters significantly affect the stress state within reinforced concrete shear walls. Similarly, Merabti et al. [29] reported that the size of openings should be limited according to the wall thickness t : for $t = 25$ cm, the opening length should not exceed $6t$; for $t = 20$ cm, it should remain below $8t$; and for $t = 15$ cm, it should range between $11t$ and $13t$.

Despite the extensive literature devoted to reinforced concrete shear walls, the effect of L-shaped shear wall layout on the global seismic response of buildings remains insufficiently

documented and inadequately quantified. This study, therefore, investigates the influence of the positioning of L-shaped shear walls with constant geometry and thickness on lateral stiffness, stress distribution, and overall seismic demand of the structure. To address this issue, a numerical modeling campaign is conducted by comparing several layout configurations using key response indicators, including lateral displacements, base shear, overturning moments, and stress levels in the shear walls.

2. STUDIED MODELS

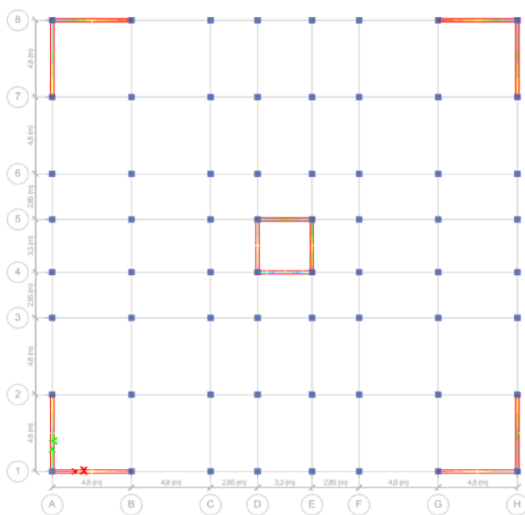
Four building configurations were investigated (Figure 1), each corresponding to a ten-story reinforced concrete structure with a ground floor, located in a high seismicity area (Zone III) in accordance with the Algerian seismic code

RPA99/2003 [8]. Each model is laterally braced by reinforced concrete L-shaped shear walls with a constant thickness of 20 cm, while their layout varies from one configuration to another.

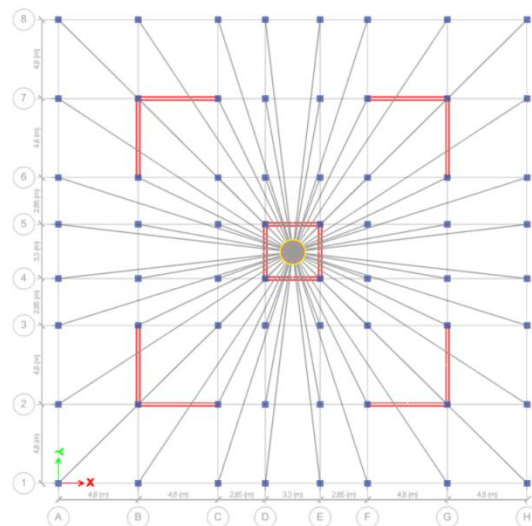
The selected layouts were defined to ensure globally comparable stiffness in the two principal directions (x and y), while maintaining geometric symmetry. This approach aims to isolate the effect of the geometry and positioning of L-shaped shear walls on the overall structural response, to identify the configuration offering the best seismic performance. Table 1 presents the adopted dimensions of columns and beams, whereas the story height is kept constant at 3.06 m for all models.

Table 1: Reinforced concrete element characteristics (cm x cm)

Storeys	Section of Column	Main beams	secondary beams
Storey: 1	50x50	30x45	30x45
Storey: 2, 3, 4	45x45	30x45	30x45
Storey: 5, 6, 7	40x40	30x45	30x45
Storey: 8, 9, 10, 11	35x35	30x45	30x45



Model 1



Model 2

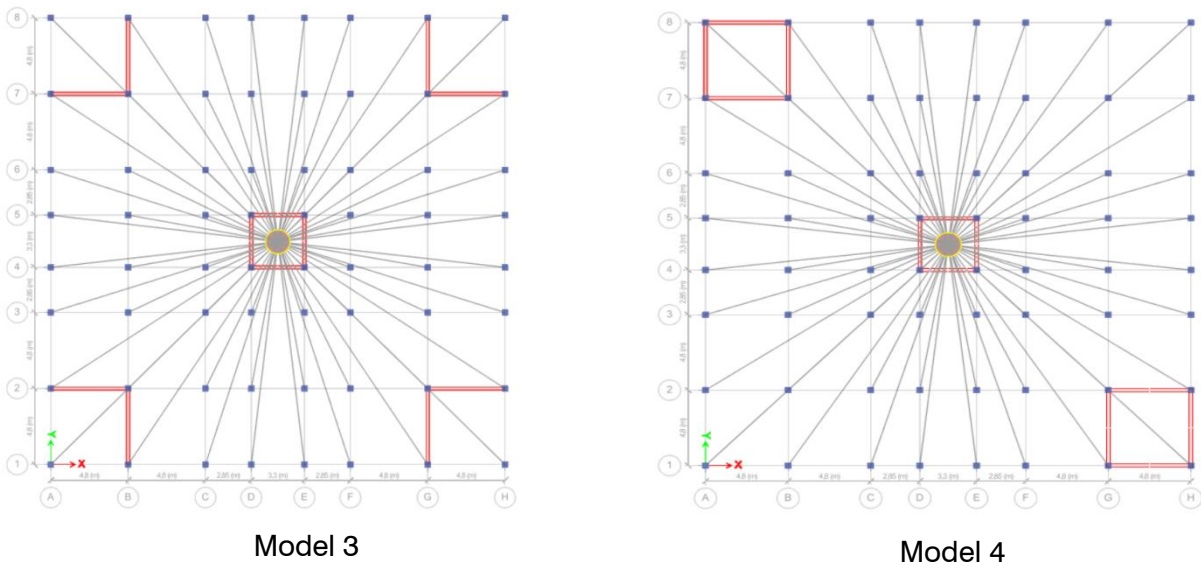


Fig. 1: Comparative L-shaped shear wall layout

.3. MATERIAL PARAMETERS AND LOAD CASES

The concrete used in all buildings has a unit weight of 25 kN/m³, a characteristic compressive strength $f_{ck}=25$ MPa, and an elastic modulus $E_c=32164.2$ MPa. The Poisson's ratio of concrete is taken as $\nu=0.2$. The reinforcing steel has a unit weight of 77 kN/m³, an elastic modulus $E_s=200$ GPa, and a Poisson's ratio $\nu=0.30$. The gravity loads generally include the permanent load G, estimated at 5.23 kN/m² for typical floors and 6.77 kN/m² for the roof, as well as the live (imposed) load Q, set at 1.5 kN/m² for typical floors and 1.0 kN/m² for the roof. These values are established in accordance with the requirements of DTR BC 22 [30]. However, the assessment of structural behavior focuses primarily on the effects of lateral loads, particularly those induced by seismic actions.

For the calculation of the seismic weight, the adopted load combination is $WG+0.2WQ$, in compliance with RPA99/v2003 [8].

$$\sigma_{1,2} = \frac{N}{A} \pm \frac{M.V}{I} \leq \bar{\sigma} \quad (1)$$

Where:

- A: cross-sectional area of the sail.
- I: moment of inertia.
- N: normal force applied.
- M: bending moment applied.
- V: distance between the centre of gravity of the sail and the furthest fibre
- $\bar{\sigma} : 0.6 f_{c28} \quad (f_{c28}=25\text{MPa})$

The shear stress in the sails is usually evaluated using equations 2 and 3.

$$\tau_b = \frac{\bar{T}}{b_0 \cdot d} \leq \bar{\tau}_b \quad (2)$$

$$\bar{T} = 1.4T \quad (3)$$

Where:

- T: Shear force due to earthquake.
- b_0 : Thickness of the wall
- d: 0.9h
- h: Total height of the section
- $\bar{\tau}_b \leq 0.2 f_{c28}$

4. RPA SEISMIC DESIGN CRITERIA

The seismic action is modeled using a horizontal response spectrum with 10%

damping. Under RPA 99/2003[8], this spectrum is defined by Equation (4).

$$\frac{S_a}{g} = \begin{cases} 1.25A \left(1 + \frac{T}{T_1} \left(2.5\eta \frac{Q}{R} - 1 \right) \right) & 0 \leq T \leq T_1 \\ 1.25A \cdot (2.5\eta) \left(\frac{Q}{R} \right) & T_1 \leq T \leq T_2 \\ 1.25A \cdot (2.5\eta) \left(\frac{Q}{R} \right) \left(\frac{T_2}{T} \right)^{2/3} & T_2 \leq T \leq 3 \text{ s} \\ 1.25A \cdot (2.5\eta) \left(\frac{Q}{R} \right) \left(\frac{T_2}{3} \right)^{2/3} \left(\frac{3}{T} \right)^{5/3} & T > 3 \text{ s} \end{cases} \quad (4)$$

where S_a/g denotes the ordinate of the acceleration response spectrum, and the seismic parameters are provided in Table 2. The parameter η represents the damping correction factor, given by Equation 4.

$$\eta = \sqrt{\frac{7}{2(2 + \xi)}} \geq 0.7 \quad (5)$$

ξ : Damping ratio (%)

Table 2: Parameters applied to buildings

Seismic parameters	Symbols	Values
Acceleration coefficient of the zone	A	0.25
Characteristic period of S2 soil (sec)	T1	0.15
Characteristic period of S2 soil (sec)	T2	0.40
Quality factor	Q	1.15
Behaviour factor	R	4.00
Damping ratio (%)	ξ	10
Damping correction factor	η	0.88

$$D = \begin{cases} (2.5\eta) & 0 \leq T \leq T_2 \\ (2.5\eta) \left(\frac{T_2}{T} \right)^{2/3} & T_2 \leq T \leq 3.0 \text{ s} \\ (2.5\eta) \left(\frac{T_2}{3} \right)^{2/3} \left(\frac{3}{T} \right)^{5/3} & T > 3 \text{ s} \end{cases} \quad (7)$$

In this study, the total seismic force, or base shear (V), applied at the foundation level, is determined successively in the two principal directions of the building, in accordance with Equation (6) prescribed by RPA99/2003 [8].

$$V = \frac{A \cdot D \cdot Q}{R} \times W \quad (6)$$

The various parameters involved in the evaluation of this static seismic force are summarized in Table 2. The average dynamic amplification factor, however, depends on the site category, the damping correction factor (η), and the fundamental period of the structure (T) (see Equation 7).

The values of D adopted in this study are 1.73 for the building without shear walls and 1.50 for buildings equipped with shear walls.

In the case of a three-dimensional analysis, in addition to the calculated theoretical eccentricity, an accidental eccentricity equal to $\pm 0.05 L$ is considered, where L is the floor dimension perpendicular to the seismic direction.

The fundamental period T of a structure can be estimated using empirical formulas, analytical approaches, or numerical modeling methods. In this study, T is evaluated using the empirical

formula (8), in accordance with the provisions of RPA99, revised in 2003 [8].

$$T = \min \begin{cases} T = 0.09 \frac{h_N}{\sqrt{D}} \\ T = C_T x h_N^{3/4} \end{cases} \quad (8)$$

Where:

- $C_T=0.05$
- h_N : Height of the structure measured in meters up to the topmost level, which is 33.66 m
- D : Dimension of the building measured at its base in the considered calculation direction, equal to 28.20 m in both directions

5. RESULTS AND DISCUSSION

5.1. Lateral displacement

The lateral displacements obtained for each model, as a function of the number of stories, are shown in Figure 2. Examination of the results indicates that Model 4 exhibits the lowest drifts in the x-direction, whereas Model 3

shows the highest values. A similar overall hierarchy is observed in the y-direction. Moreover, the displacements measured along the x-direction are generally higher than those along the y-direction.

This directional difference can be attributed to stiffness asymmetry associated with the arrangement of shear walls around the elevator core. In particular, the presence of an opening in this area locally reduces lateral stiffness, resulting in a moderate increase in displacements. Finally, a reduction in top-story displacement of approximately 14% is observed for Model 4 compared to Model 2 in the x-direction, and about 13% in the y-direction, highlighting the effectiveness of the Model 4 configuration in controlling the lateral response.

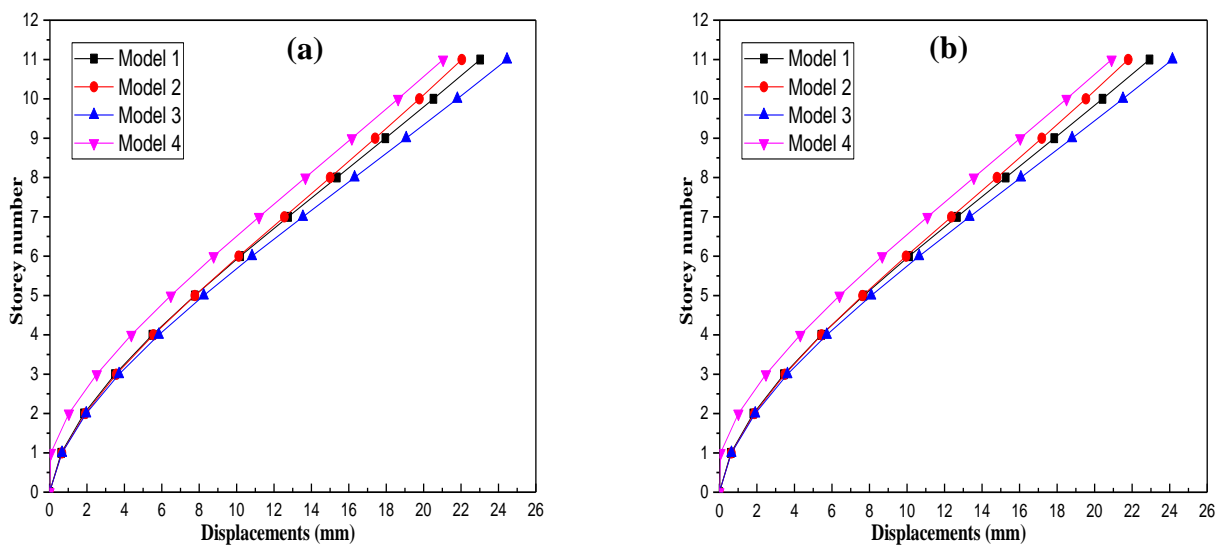


Fig. 2: Lateral displacements of the different building models as a function of the number of stories: (a) x-direction, (b) y-direction

5.2. Base shear forces

The base shear forces were evaluated in both principal directions (x and y), as shown in Figure 3. Among the analyzed configurations, Model 4, characterized by two corner cores and a central core, exhibits the lowest base shear values in both directions. The results then increase in the following order: Models 3, 1, and 2, highlighting the effectiveness of the Model 4 layout in reducing seismic demands.

It is also noteworthy that, despite an overall symmetrical geometry, the base shear remains higher in the x-direction than in the y-direction. This difference can be attributed to local features, particularly the opening at the elevator core, which may reduce lateral stiffness in the x-direction. Finally, the comparison reveals a reduction of approximately 16% in base shear for Model 4 compared to Model 2 in the x-direction, and about 13% in the y-direction, confirming the decisive influence of shear wall distribution on the overall seismic performance of the structure.

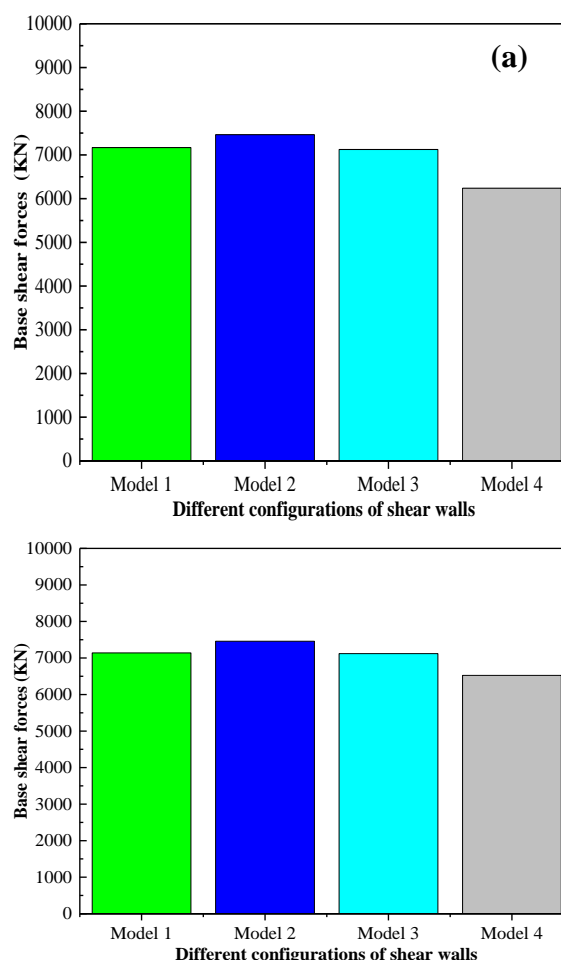


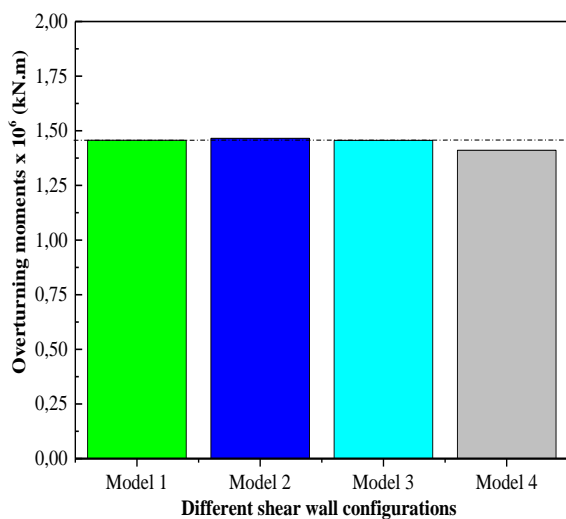
Fig. 3: Base shear forces of the different models: (a) x-direction, (b) y-direction

5.3. Overturning moments of the buildings

For each configuration, the overturning moments of the buildings were evaluated in both principal directions, as shown in Figure 4. The results indicate that Model 4 remains the most efficient in both the x- and y-directions, exhibiting the lowest overturning moments among all analyzed configurations. However, it should be noted that the values obtained for the

(a)

four models are relatively close.



For instance, the overturning moment of Model 4 is approximately 3% lower than that of Model 2 in the x-direction, the latter generating the highest values. In terms of overall performance, a ranking can be established as follows: Model 4 ranks first, followed by Models 3, 1, and finally

2. These findings confirm the effectiveness of the layout adopted in Model 4 for enhancing the overall stability of structures under seismic loading.

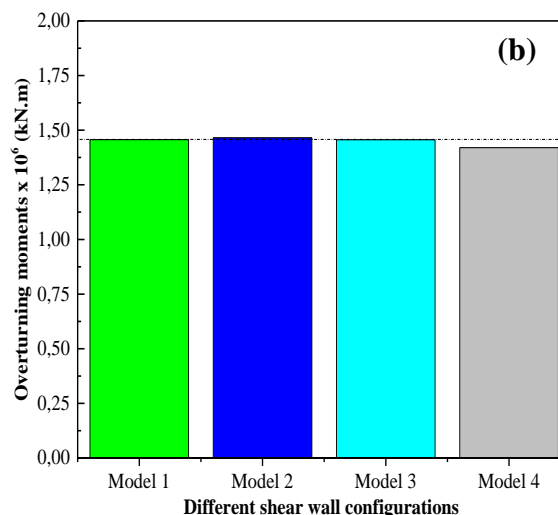


Fig. 4: Overturning moments for the various building models:
 (a) in the x-direction, (b) in the y-direction

5.4. Shear stresses in the walls

The maximum shear stresses developed in the L-shaped shear walls of Model 1 were analyzed in the x-direction under the load combination $G+Q \pm Ex$ (where Ex represents the seismic force in the x-direction). The highest value, reaching 3.5 MPa, is observed at the ground floor, specifically in the elevator core area. This stress concentration occurs primarily at the lintel, highlighting the critical role of this element in transferring seismic forces and emphasizing the need for locally reinforced reinforcement. Additionally, a shear stress of approximately 1.56 MPa is observed in another region of the L-shaped wall. Overall, the stresses tend to decrease with building height. The more pronounced demand in the x-direction can be attributed to the presence of an opening in the

elevator core, which locally reduces stiffness. Nevertheless, all values remain below 5 MPa, generally accepted as an allowable limit in standard seismic design practice.

For Model 2, the maximum shear stress in the L-shaped wall along the x-direction reaches 1.66 MPa, representing an increase of about 6% compared to Model 1. In contrast, the maximum stress measured at the central core lintel is 3.25 MPa, corresponding to a reduction of approximately 7% relative to the previous case, indicating a partial redistribution of forces. In Model 3, the shear stress in the L-shaped wall is slightly lower, at 1.60 MPa, confirming a moderate decrease compared to Model 2. However, the maximum stress remains concentrated at the lintel, with a stable value of 3.25 MPa, reflecting the persistent sensitivity of this region to seismic effects.

Model 4, however, stands out with the lowest stress levels among all configurations studied. The maximum stress recorded in the L-shaped wall is 1.45 MPa, located on the first floor, while the stress at the lintel, also on the first floor, reaches 2.80 MPa. This notable reduction compared to the other models demonstrates a better distribution of internal forces and a significant mitigation of critical stress concentrations.

Overall, these results indicate that the configuration adopted in Model 4 promotes a more uniform distribution of shear forces within the walls while limiting excessive concentrations at the lintels. This layout thus contributes to an overall improvement in the seismic performance of the structure.

5.5. Compressive and tensile stresses in the walls

The maximum compressive stress reaches 10.49 MPa and is concentrated at the ground floor, primarily at the ends of the L-shaped walls. It then decreases with height, reflecting the progressive redistribution of vertical loads and seismic forces along the building. Among the examined load combinations, $G+Q \pm Ex$ proves the most critical, producing the highest compressive stress levels. Nevertheless, the maximum value remains below the allowable limit of 15 MPa, indicating that safety criteria are satisfied.

Regarding tensile stresses, the highest value is 3 MPa, occurring at the top floor, at the lintel. This upper-level location highlights a potentially critical area under seismic loading, warranting specific verification of the element for both shear and induced tensile forces to ensure safety and durability.

For Model 2, the maximum compression remains at the ends of the L-shaped wall, reaching 10.85 MPa, representing an increase of about 3% compared to Model 1. The maximum tensile stress remains unchanged (3 MPa) and is observed at the top level near the central core.

Model 3 exhibits slightly higher compression (10.96 MPa), located at the ends of both wings of the L-shaped wall. The maximum tensile stress measured at the central core on the top floor reaches 3.46 MPa, approximately 15% higher than in Models 1 and 2, indicating an intensification of tensile effects and requiring particular attention to these sensitive areas under seismic load combinations.

Finally, Model 4 stands out with a significant reduction in maximum compressive stress, limited to 6.71 MPa at the ground floor, suggesting a better distribution of compressive forces. In contrast, the maximum tensile stress increases to 4 MPa at the top floor in the central core area; thus, despite the improvement in compression, this model requires careful design and reinforcement of the upper core zones, particularly for lintel-type elements subjected to combined actions.

6. CONCLUSION

The comparative study of the four reinforced concrete L-shaped shear wall configurations highlights marked differences in the overall seismic response depending on the adopted layout. The assessment focused on several performance indicators, including internal stresses (shear, compression, and tension), base shear, overturning moments, and lateral displacements.

In terms of shear, Model 4 stands out with the lowest levels, both in the walls (1.45 MPa) and

at the lintels (2.80 MPa), reflecting a more uniform mobilization of the resisting system. In contrast, Model 1 exhibits the highest shear stress at the lintel (3.5 MPa), suggesting the presence of a highly stressed and potentially critical zone.

Regarding compression, Models 1 to 3 display very similar values (ranging from 10.49 to 10.96 MPa), concentrated at the ground floor at the wall ends, corresponding to the classically most compressed regions. Model 4, however, records a significantly lower maximum stress (6.71 MPa), indicating a better redistribution of compressive forces. For tensile stresses, the maximum occurs in Model 4 (4 MPa at the top floor), suggesting that tensile demands are more significantly transferred to the upper portions of the structure.

The analysis of base shear confirms the superior performance of Model 4, which exhibits the lowest values in both directions (x and y), followed by Models 3 and 1, while Model 2 remains the least favorable. The difference between Models 4 and 2 reaches approximately 16% in the x-direction and 13% in the y-direction, highlighting the direct influence of core/wall layout on the overall seismic demand.

For overturning moments, differences are less pronounced, yet Model 4 maintains an advantage, with a reduction of about 3% compared to Model 2, considered the most critical case. Finally, the examination of lateral displacements shows that Model 4 is the most effective in controlling drifts, with reductions of approximately 14% in the x-direction and 13% in the y-direction compared to Model 2, whereas Model 3 produces the highest displacements.

Overall, Model 4 emerges as the most favorable solution across all considered criteria, offering a

robust compromise between stiffness, force distribution, and mitigation of critical demands. These trends indicate that combining corner cores with a central core represents an effective strategy to enhance the seismic bracing of medium- to high-rise reinforced concrete structures and can inform practical recommendations in seismic design engineering.

5. ACKNOWLEDGEMENTS

The authors gratefully acknowledge the support and contributions of their colleagues and laboratory members

6. REFERENCES

- [1] Boudina, A., Merabti, S., Benyamina, S., Guettiche, A., Chadouli, R. Impact of the evolution of the RPA 2024 seismic code and major earthquakes on the seismic response of self-stable reinforced concrete buildings. *Research on Engineering Structures & Materials*, 1-19. 2025.
- [2] Khelladi, Benyamina, M and Merabti, S, (2024) Influence of Empirical and Dynamic Periods on the Seismic Responses of Reinforced Concrete Buildings Braced by L-Shaped Shear Walls. *The Journal of Engineering and Exact Sciences*. 10 (4), 18672-18672. <https://doi.org/10.18540/jcecvl10iss4pp18672>.
- [3] F. Dashti, R.P. Dhakal, S. Pampanin. Numerical modeling of Rectangular Reinforced Concrete Structural Walls, *J Struct Eng*. 143 (2017). 04017031
- [4] Pilakoutas, K. Elnashai. A.S. Cyclic behavior of reinforced concrete cantilever walls, Part II: Discussions and theoretical comparisons, *ACI Struct. J*. 92 (1995). Pp 425-434.

- [5] Merabti S. Influence of the suppression of the corner column on the compressive stresses of L-shaped rc shear walls. *Brazilian Journal of Production Engineering* 10 (4), 164-138-147.2024.
- [6] Zhou, Y., Zhu, X., Wu, H., Gu, A., Wenbo, T. (2023). Seismic design and engineering practice of a 10-story self-centering precast concrete wall structure, *Structural Design of Tall and Special Buildings*,
- [7] V.N. Varma. U.P Kumar. Seismic response on multi-storied building having shear walls with and without openings, *Mater Today: Proceedings*. (2021). 37(2).801-805
- [8] DTR B.C2-48 (Regulatory Technical Document). (2003). Ministry of Habitat. Algerian Paraseismic Regulations, RPA 99/Version 2003, National Center for applied research in paraseismic engineering, Edition CGS, Algeria.
- [9] EN 1998-1:2004 (Eurocode 8): Design and dimensioning of structures for resistance to earthquakes. European Committee for Standardisation.
- [10] Merabti, S., Guelmine, L., Kaci, M. Parametric analysis of the seismic behavior of reinforced concrete shear walls in buildings: application of the pushover method. *Romanian Journal of Materials/Revista Romana de Materiale*. 55 (2). 2025.
- [11] Merabti S. A comparative simulation study of the effect of column suppression on shear stress in an L-shaped RC wall with openings. *Brazilian Journal of Production Engineering* 11 (3), 316-327.2025.
- [13] Merabti, S.,Yahiaoui, I., Mezidi, A and Guelmine, L. Numerical investigation of shear stress in buildings reinforced by walls without corner columns. *South Florida Journal of Development* 6 (1), e4916-e4916.2025.
- [14] Dehghani, S and Tobber, L. (2024). Implications of the 2020 National Building Code of Canada updates on the design demands for reinforced concrete shear wall buildings. *Canadian Journal of Civil Engineering*. 51 (8), PP. 858-873.
- [15] Zhou, Y., Fan, L., Xing, F., Lin, W., Rui, H., Guo, M and Zhu. Z. (2024). Effect of nano-SiO₂ modification on the seismic performance of recycled aggregate concrete shear walls. *Engineering Structures*. V 307, 117945.
- [16] Merabti, S., Bezari, S., Aymen, A., and Khachouche, A. (2023). Investigation into the Impact of L-Shaped RC Shear Wall Placement with Openings on the Behavior of Medium-Rise Buildings. *The Journal of Engineering and Exact Sciences*, 09 (09).
- [17] Reydson de Barros, S., Bernardo Horowitz, J and Filipe Almeida Bernardo, L. (2023). Nonlinear analysis of planar, H-shaped and U-shaped thin reinforced concrete shear walls. *Structures*. 49, PP. 295-311. <https://doi.org/10.1016/j.istruc.2023.01.117>
- [18] Merabti, S. Combined effect of removing corner columns and vertical openings in an L-shaped shear wall. *Studies in Engineering and Exact Sciences* 5 (2), e11381-e11381.2024. <https://doi.org/10.54021/seesv5n2-602>.
- [19] Boudina, A., Merabti, S., Benyamina, S., Guettiche, A., Chadouli R. Impact of the evolution of the RPA 2024 seismic code and major earthquakes on the seismic response of self-stable reinforced concrete buildings. *Research on Engineering Structures & Materials*, 1-19. 2025.

- [20] Merabti, S., and Bezari, S. (2023). Study of Stress Distribution in L-Shaped Walls with Openings under Intense Seismic Conditions on Various Soil Types. *The Journal of Engineering and Exact Sciences*, 9(8).
- [21] Ma, J., Kang, S-B and Li. B. (2019). Influence of shear span ratio on the seismic performance of L-shaped RC walls. *Magazine of Concrete Research*. 73(1), PP.32-44..
- [22] Ahmed-Chaouch, A., Bechtoula, H and Bali, A. (2016). A Comparative Numerical Study on Shear Stress Variation of an L Shaped RC Wall With and Without Corner Column. *Wulfenia Journal*. 23(10).
- [23] Ozkula, T.A., Kurtbeyoglu, A., Borekcic, M., Zengind, B and Kocakc, A. (2019). Effect of shear wall on seismic performance of RC frame buildings. *Engineering Failure Analysis*. 100. PP. 60-75.
- [24] Zhang, P., Wang, J and Gao, J. (2022). Cyclic Behavior of L-Shaped RC Short-Limb Shear Walls with High-Strength Rebar and High-Strength Concrete. *12 (16)*, 8376.
- [25] Yang, Y., Huang, L., Xu, L., Gao, H., Yu, M and Chi, Y. (2024). A bottom-up analysis of the seismic performance of prefabricated recycled concrete shear wall via concurrent macro-mesoscale numerical approach. *Construction and Building Materials*. 415, 135037.
- [26] Zhou, Y., Lin, W., Hu, R., Xing, F., Guo, M., Zhuang, J and Xu. W. (2024). Seismic performance of carbonated recycled aggregate concrete shear walls. *Construction and Building Materials*. 443, 137633.
- [27] Ding, Y., Zhou, Z., Wei, Y and Zhou, S. (2024). Experimental study and efficient shear-flexure interaction model of reinforced concrete shear walls with UHPC boundary columns. *Case Studies in Construction Materials*. 20, e03059.
- [28] Kalpana, P. Prasad, R.D. Kranthi Kumar, B. Analysis of Building with and without Shear Wall at various Heights and Variation of Zone III and Zone V, *Int J Eng Res. Appl.* 8 (2016) 631–635.
- [29] Merabti S, Guelmine L, Afkir M, Fekir Z. Numerical simulation of the behavior of L-shaped RC shear walls with staggered openings. *Brazilian Journal of Production Engineering* 10 (3), 164-173.2024.
- [30] D.T.R. (Document Technique Réglementaire) BC 2.2. Permanent loads and live loads. Algeria: National Center for Applied Research in Paraseismic Engineering; 1988.